RECORDSOF CHEMICAL SCIENCES

Accepted: 15th Nov, 2024
Published: 16th Dec, 2024

Molecular Docking and Dynamics Studies of Novel Pyrrolone Derivatives as Promising Inhibitors of *Plasmodium falciparum*.

[1]Zaharaddeen Shehu, [2, 3]Saudatu Chinade Ja'afaru, [3]Adamu Uzairu, [4]Muhammad Yahaya, [5]Mohammed A. A., [6]Sani Iliya, 7Jonathan Mwangi, [8]Ronald Maathai, [9]Mary Muruiki Hutchins, [10]Muhammad I. H

1. Department of Science Laboratory Technology, Jigawa State Polytechnic, Dutse, Jigawa State 2. Department of Chemistry, Aliko Dangote University of Science and Technology Wudil, Kano Satate. 3. Department of Chemistry Ahmadu Bello University Zaria, 4. Department of Chemical Pathology, Rasheed Shekoni Federal University Teaching Hospital, Dutse 5. Department of Chemistry Jigawa State College of Education Gumel, 6. Department of Biological Sciences, School of Pure and Applied Sciences, Mount Kenya University Thika, Thika, Kenya. 7.School of Pharmacy and Health Sciences, United States International University-Africa, Nairobi Kenya. 8. Department of Biochemistry, Mount Kenya University, Thika Kenya. 9.Department of Chemistry, School of Science and Engineering, Saint Louis University, Missouri, USA. 10. Department of Remedial and General Studies, Audu Bako College of Agriculture, Danbatta.

*Corresponding Author:
Zaharaddeen Shehu.
zshehu@jigpoly.edu.ng

FRsCS Vol. 3 No. 4 (2024)
Official Journal of Dept. of Chemistry, Federal University of Dutsin-Ma, Katsina State.
http://rudmafudma.com

ISSN (Online): 2705-2362
ISSN (Print): 2705-2354

https://doi.org/10.33003/frscs_2024_0304/05

Abstract

Malaria continues to be a significant global health challenge, with 247 million cases and 619,000 deaths reported in 2022, primarily in sub-Saharan Africa, underscoring the urgent need for effective therapies. This study investigates the potential of pyrrolone derivatives as novel inhibitors of Plasmodium falciparum dihydrofolate reductase-thymidylate synthase (PfDHFR-TS) for malaria treatment. Using a structure-based drug design approach, 38 known pyrrolone derivatives with potential against PfDHFR-TS were screened to identify a lead candidate for the development of new potential drug candidates with improved binding affinity. Compound 31 was selected as the lead compound, and docking simulations guided the design of six new inhibitors. Among these, compound D5 exhibited the highest binding score of -172.577 kcal/mol, a Re-rank score of -132.753 kcal/mol, and a hydrogen bond energy of -9.550 kcal/mol. A 100-ns molecular dynamics (MD) simulation further revealed that compound D5 showed stronger binding affinity and greater stabilizing potential compared to the apo-protein, as indicated by root mean square deviation (RMSD), root mean square fluctuation (RMSF), radius of gyration (Rg), and Solvent Accessible Surface Area (SASA) analyses. Additionally, the designed compounds displayed promising pharmacokinetic profiles based on drug-likeness and ADMET property studies. Consequently, these compounds have potential as novel PfDHFR-TS inhibitors, pending further preclinical and clinical studies to verify their efficacy and safety.

Keywords: Malaria; *Plasmodium falciparum*; Drug design; Molecular docking; DFT.

Introduction

Malaria remains one of the world's most significant public health concerns, affecting millions of lives each year (Talapko et al., 2019). According to the World Health Organization (WHO), there were an estimated 247 million malaria cases globally in 2022, with the disease causing 619,000 deaths (Lartey, 2024; Garrido-Cardenas 2023). The vast majority of cases and deaths occurred in sub-Saharan Africa, highlighting the disproportionate burden borne by this region (Kolawole et al., 2023; Kogan et al., 2020). Children under five and pregnant women are particularly vulnerable to severe forms of the disease, making it a leading cause of childhood mortality in these areas. In Nigeria, malaria's impact is even more pronounced. The country accounts for approximately 27% of global malaria cases and 32% of malaria-related deaths, making it the highest-burden nation worldwide (Oladoyinbo, 2018; Yahaya, 2022). In 2021 alone, Nigeria reported over 68 million cases and nearly 194,000 deaths due to malaria (Nuga et al., 2024). This staggering burden strains the healthcare system and significantly impacts economic productivity, with malaria cited as a major cause of absenteeism and economic losses across sectors. Efforts to combat malaria in Nigeria include extensive distribution of insecticide-treated nets (ITNs), enhanced surveillance, and the rollout of new malaria vaccines (Okumu, et al., 2022). However, challenges such as low ITN utilization and drug resistance continue to hamper progress. Addressing these barriers remains critical to achieving the goal of malaria elimination both in Nigeria and globally.

Current malaria treatments face significant challenges that necessitate the development of alternative therapies (Obeagu & Obeagu, 2024a). Drug resistance, especially to Artemisinin-based combination therapies (ACTs), threatens the efficacy of frontline medications, with resistant strains increasingly reported in parts of Africa and Southeast Asia (Waweru, 2024; Alghamdi et al., 2024). Access to high-quality treatments is limited in low-resource regions like Nigeria due to economic barriers and the prevalence of fake drugs. Existing therapies often fail to address dormant liver-stage parasites, leading to relapses, and they can also cause adverse effects, reducing patient compliance (Alghamdi et al., 2024). Moreover, treatments specifically designed for vulnerable populations, such as pregnant women and children, remain limited (Obeagu & Obeagu, 2024b). Logistical difficulties in distributing treatments and preventative tools further hinder malaria control efforts. Therefore, designing alternative therapies with novel mechanisms of action and the ability to target all parasite life stages is crucial to overcoming these barriers.

Plasmodium falciparum dihydrofolate reductase-thymidylate synthase (PfDHFR-TS) is a highly preferred protein target for computer-aided drug design (CADD) against malaria due to its essential role in the parasite's survival and replication (Khelfa, 2024). This bifunctional enzyme is central to the folate pathway, catalyzing the reduction of dihydrofolate to tetrahydrofolate (DHFR activity) and the synthesis of thymidylate from deoxyuridylate (TS activity), both critical for DNA synthesis and cell replication (Loh, 2023; Marttila, 2023). Inhibiting PfDHFR-TS disrupts these processes, ultimately leading to parasite death. Its role as a validated drug target is reinforced by the effectiveness of existing antimalarial drugs like proguanil, which inhibit PfDHFR-TS (Ojha, 2021). However, resistance to these drugs due to mutations in the enzyme highlights the need for novel inhibitors. The structural differences between PfDHFR-TS and its human counterpart enable selective targeting, reducing off-target effects and toxicity. Additionally, the availability of high-resolution crystal structures of PfDHFR-TS facilitates structure-based drug design, allowing for efficient *in silico* screening and optimization of potential inhibitors. Computer-aided drug design (CADD) approaches, such as molecular docking and molecular dynamics simulations, provide tools to design molecules that can overcome resistance mutations and achieve high efficacy (Nascimento et al., 2022; Bassani & Moro, 2024). Furthermore, PfDHFR-TS inhibitors have significant potential for interaction when combined with other antimalarials, enhancing their overall therapeutic impact (Oluyemi et al., 2024; Shamshad et al., 2022). Notably, the traditional trial-and-error method in experimental drug discovery is both time-consuming and resource-intensive (Tiwari et al., 2023). To address these challenges, theoretical models and computational techniques have been employed. Computer-aided drug design (CADD) offers valuable perceptions into protein-ligand interactions and binding affinities. In this study, structure-based drug design (SBDD) was utilized to identify derivatives with improved binding efficacy (Fischer et al., 2024). This approach incorporated molecular docking, molecular dynamics (MD) simulations, ADMET property predictions and Density Functional Theory (DFT) calculations. The primary aim was to design, identify and evaluate promising pyrrolone derivatives as potential inhibitors for malaria. The findings of this research demonstrate encouraging potential for the development of novel therapeutic options for malaria, meeting the urgent need for more effective treatment options against this illness.

Methodology

Data Acquisition, Structural Analysis, and Optimization

A set of thirty-eight pyrrolone derivatives, identified as potential PfDHFR-TS inhibitors, was sourced from the literature (Murugesan et al., 2013). The 2D molecular structures of these derivatives were generated using ChemDraw software, adhering to the ACS Document 1996 guidelines to ensure compliance with industry standards (Table 1) (Hassan et al., 2022; Thomsen & Christensen, 2006). These 2D structures were converted into 3D formats using Spartan 14 software, and their geometric energy was initially minimized using molecular mechanics force fields (MMFF) (Ameji &Uzairu, 2024). To enhance precision, the minimized structures were further optimized using Density Functional Theory (DFT) calculations with the B3LYP/6-31G* basis set, resulting in more reliable conformers (Sert et al., 2020). The optimized conformers were saved in sdf and pdb formats to facilitate molecular docking studies and the calculation of quantum chemical reactivity descriptors.

Receptor Identification, Preparation and Molecular Docking Studies

The Molegro Virtual Docker (MVD) software was utilized to perform molecular docking analysis between the identified pyrrolone derivatives and the active site of PfDHFR-TS (PDB ID: 7F3Y) in order to explore and identify potential lead compounds for anti-malarial inhibitor design through structure-based drug design (SBDD) (Maurya, et al., 2020). Prior to docking, the target protein was prepared in the Discovery Studio workspace by removing water molecules and co-crystallized ligands. The modified target protein was then loaded into MVD for docking analysis.

Table 1: Molecular structures and biological activities of Pyrrolone derivatives

S/N	Molecular structure	pIC_{50}	S/N	Molecular structure	pIC_{50}
1	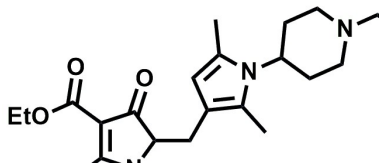	7.456	**20**	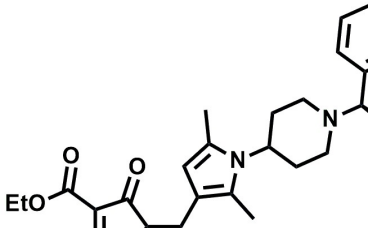	9.000
2	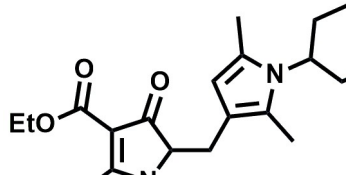	4.921	**21**	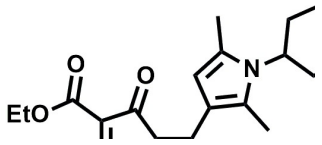	5.276
3	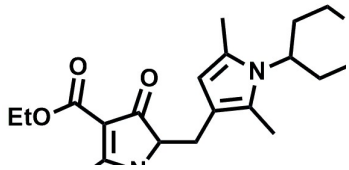	5.854	**22**	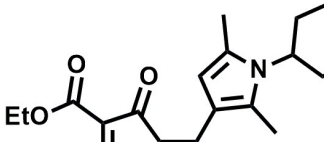	5.620
4	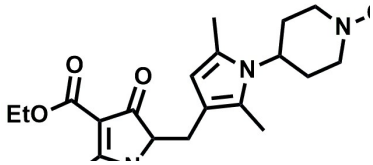	5.62	**23**	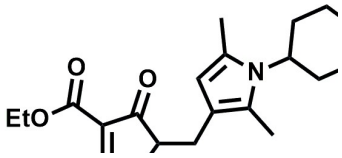	5.456
5	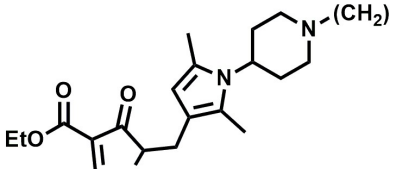	6.721	**24**	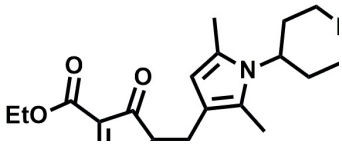	7.796
6	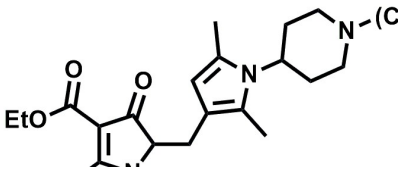	5.959	**25**	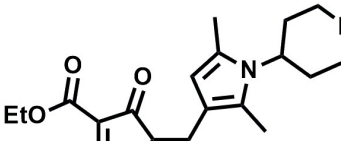	6.959

7	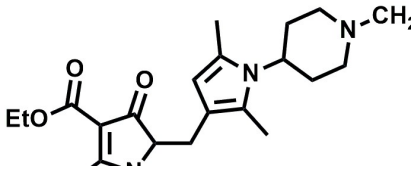	7.237	**26**	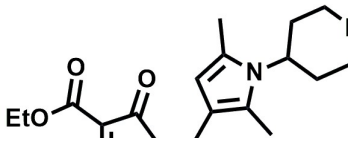	5.854
8	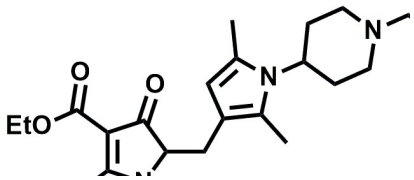	6.42	**27**	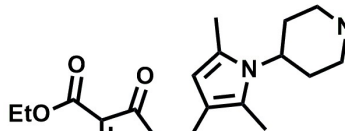	8.398
9	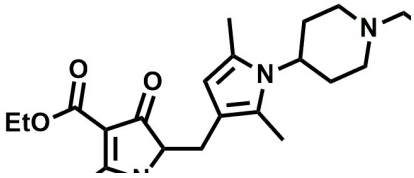	6.337	**28**	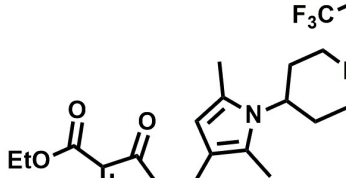	9.398
10	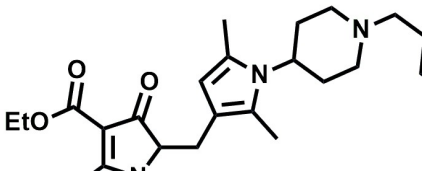	7.62	**29**	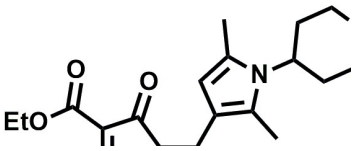	6.824
11	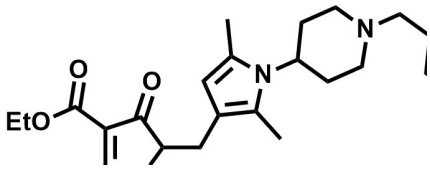	7.638	**30**	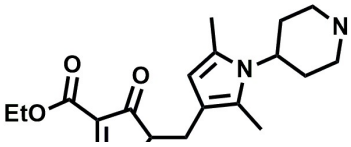	5.921
12	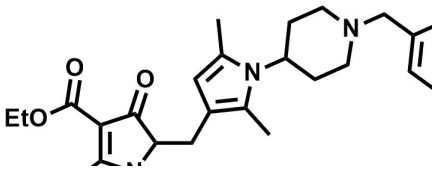	8.699	**31**	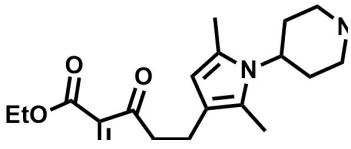	7.000

13	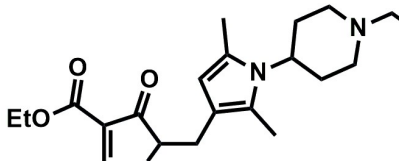	9.301	**32**	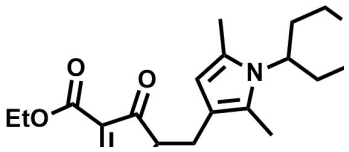	7.745
14	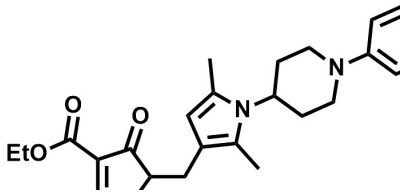	7.62	**33**	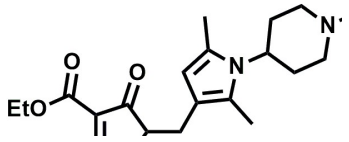	6.000
15	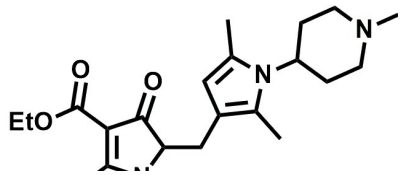	6.495	**34**	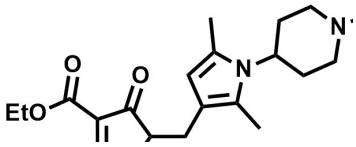	7.921
16	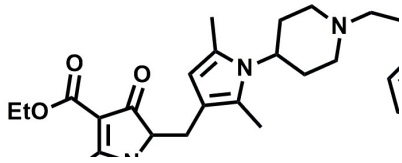	7.081	**35**	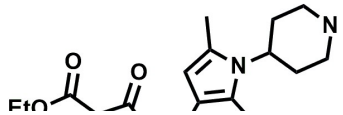	9.000
17	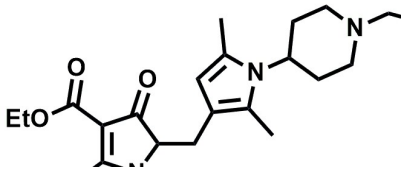	6.886	**36**	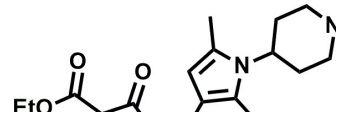	5.824
18	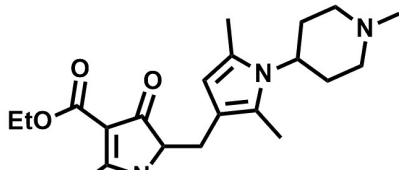	7.018	**37**	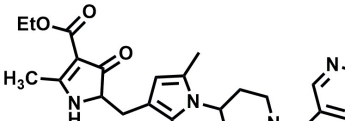	7.125
19	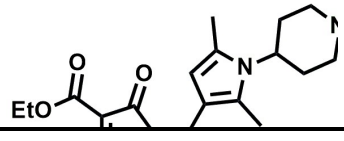	8.155	**38**	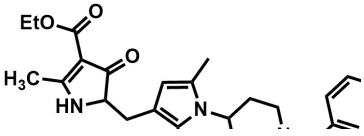	5.585

An electrostatic surface map was generated, and five potential binding cavities were identified. The optimized derivatives (ligands) were introduced, and docking was initiated. The best binding cavity, located at coordinates XYZ 18.51, -22.04, -19.82 within a defined sphere, was selected (Shah et al., 2021). The Moldock (GRID) scoring algorithm was applied, using a default grid resolution of 0.3 Å, with 10 independent runs, each containing a maximum of 1500 iterations and a population size of 50. Default settings for pose generation and simplex evolution were used throughout. To validate the docking algorithm, the anti-malarial drug Amodiaquine was re-docked into the binding site, and residual interactions were analyzed, with the root mean square deviation (RMSD) score calculated between the re-docked and original poses (da Fonseca et al., 2024). Finally, Discovery Studio was employed to visualize the interactions within the generated complexes.

Structure-based drug design

Structure-based Drug Design (SBDD) was used to propose novel anti-malarial compounds targeting PfDHFR-TS by optimizing existing drug molecules. SBDD relies on detailed knowledge of a target's 3D molecular structure to design compounds that bind effectively, enhancing specificity and therapeutic potential (Jáafaru et al., 2024). Following the analysis of docking results, the compound with the highest Moldock score was selected as a template to design new derivatives that would exhibit stronger binding affinity and better interact with and modulate the target's function (Olaoye et al., 2024). Additionally, molecular dynamics (MD) simulations, drug-likeness assessments, ADMET properties (Absorption, Distribution, Metabolism, Excretion, and Toxicity), and Density Functional Theory (DFT) parameters of the proposed compounds were evaluated.

Molecular dynamics simulation

Molecular dynamics simulations of the protein-ligand complexes were carried out using AMBER18 software with the ff19SB force field (Smardz et al., 2024). The complexes were embedded in a cubic TIP3P water box, with a 10 Å buffer between the protein surface and the box edges. Short-range non-bonded interactions were calculated using a 12 Å cutoff. The tLEAP program was used to calculate the system's net charge, and counterions were added to neutralize it. Additionally, Na+ and Cl- ions were introduced to achieve a 0.15 M salt concentration (Khurshid, 2024). Before the simulations, each system underwent progressive energy minimization, both with and without constraints, to ensure a fully optimized enzyme-ligand complex. Constrained simulations were performed under the NVT ensemble, with the temperature gradually increased from 0 to 300 K over 1 ns. This was followed by a 5 ns equilibration phase with progressively reduced solute constraints. The final production run, lasting 100 ns, was conducted under the NPT ensemble, maintaining constant temperature (300 K) and pressure (1 atm) using the Nose-Hoover Langevin thermostat and barostat (Prasad et al., 2021). The SHAKE algorithm was used to constrain bonds involving hydrogen atoms, and long-range electrostatic interactions were calculated using the particle mesh Ewald (PME) method. A 2 fs integration time step was applied during the production phase, with snapshots recorded every 10 ns.

Drug score Evaluation

The evaluation of drug scores incorporates multiple factors, such as drug-likeness, cLogP, logS, molecular weight, and toxicity considerations, within a scoring algorithm (Li et al., 2024). This method aims to offer a quantitative assessment of the overall potential of the proposed anti-malaria drug candidates. Osiris Property Explorer was used to perform this evaluation (Mukadam & Jagdale, 2024).

ADMET predictions

After successfully docking the designed pyrrolone derivatives into the binding site of the PfDHFR-TS receptor, the compounds were evaluated for their ADMET properties to assess their potential as drug candidates for the treatment of malaria. For this analysis, the pkCSM (https://biosig.lab.uq.edu.au/pkcsm/) web tool was utilized to evaluate their ADMET profiles (Azzam, 2023).

Density functional theory analysis

Density Functional Theory (DFT) is a key computational approach for analysing the electronic structure, stability, and reactivity of compounds (Rong et al., 2020). It determines quantum chemical descriptors using energies from frontier molecular orbitals (FMOs), namely the highest occupied molecular orbital (HOMO) and the lowest unoccupied molecular orbital (LUMO). These descriptors provide insights into molecular properties and behaviour. In this study, quantum-chemical descriptors, including the energy gap ($\Delta E = E_{LUMO} - E_{HOMO}$) were calculated to assess the designed compounds' reactivity. Additionally, population analysis was performed to generate molecular electrostatic potential (MEP) surfaces, which are valuable in drug design (Guin et al., 2022). MEP analysis helps predict pharmacological properties, assess potential drug efficacy, and rationalize compound reactivity, making it a crucial tool for understanding drug candidates' behaviour.

Results and discussion

Molecular Docking Investigations

The active site of the PfDHFR-TS receptor, represented by PDB ID 7F3Y, consists of key amino acids, including ARG510, HIS551, SER511

, ASP513, GLY517, GLN509, and TYR553 (Tanramluk et al., 2022). These residues play a critical role in forming hydrogen bonds and hydrophobic interactions with PfDHFR-TS inhibitors. Figure 1 illustrates the superimposed docked complex of Amodiaquine, a standard drug, with the PfDHFR-TS receptor while Figure 2A shows the detailed active site interactions of Amodiaquine with the PfDHFR-TS receptor. Accurate ligand binding within the receptor's active site depends on precise docking, which requires careful selection of the grid box size and central coordinates. To ensure the reliability of the docking algorithm, Amodiaquine was re-docked into the receptor, yielding an RMSD value of 0.114 Å (Figure 1). This value is well within the accepted threshold of less than 2.0 Å, confirming the accuracy of the docking process (Shivanika, et al. 2020).

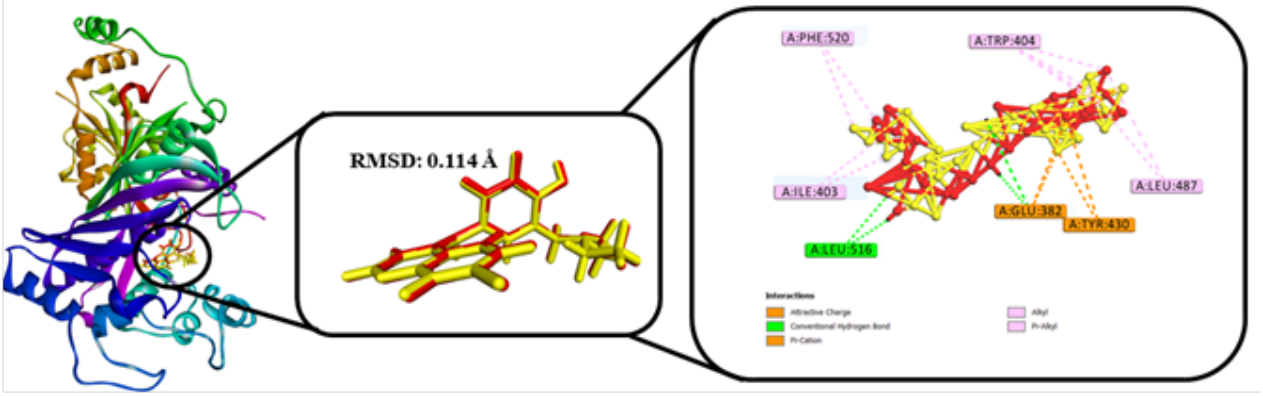

Figure 1: Visualization of the superimposed docked complex of Amodiaquine, a standard drug, with the PfDHFR-TS receptor.

Docking simulations were performed on 38 pyrrolone derivatives, identifying compound **31** as the highest binding ligand with a Moldock score of -167.319 kcal mol^{-1}, a Rerank score of -128.193 kcal mol^{-1}, and hydrogen bond energy of -5.418 kcal mol^{-1} (Table 2). This compound also showed excellent pharmacokinetic properties and was selected as the lead candidate for designing novel inhibitors with enhanced binding affinity. Its promising characteristics positioned it as the lead molecule for further drug design targeting PfDHFR-TS receptor. The binding energy scores for all 38 pyrrolone derivatives are summarized in Table 2. Compound **31**'s Moldock score with the PfDHFR-TS active site highlights the strong interaction between the ligand and receptor, while the high Rerank score underscores the stability of the docked complex. Hydrogen bond energy, crucial for maintaining ligand-receptor stability, was notable at -5.418 kcal mol^{-1}, indicating robust interactions (Abdullahi, et al., 2023). Previous studies by S.C. Ja'afaru and colleagues have emphasized that higher docking scores increase the likelihood of strong ligand binding to the receptor (Ja'afaru et al., 2023). Figure 2B provides a three-dimensional visualization of the interactions between compound 31 and the active site residues of the target protein. Five conventional hydrogen bonds were observed with ARG345, SER511, ARG510, CYS490, and TYR553, at respective distances of 2.314 Å, 1.924 Å, 1.835 Å, 2.178 Å, and 2.279 Å. Additionally, a carbon-hydrogen bond with ASN521 was noted at a distance of 3.753 Å. Several hydrophobic interactions were also identified, involving residues PRO488, LEU487, HIS491, ILE403, and PHE520. Nearly all active residues of PfDHFR-TS were encompassed within the binding site of compound 31 (Figure 2B).

Design of Potent Anti-Malaria Drugs Based on Molecular Structure

Following the virtual screening through molecular docking of 38 PfDHFR-TS inhibitors with the 7F3Y receptor, compound **31** emerged as the most promising candidate, with a MolDock score of -167.319 kcal mol^{-1}, a Re-rank score of -128.193 kcal mol^{-1}, and hydrogen bond energy of -5.418 kcal mol^{-1}. Based on these results, compound 31 was selected as the lead compound, and a design template was developed accordingly (Figure 3). Visualization of the binding interactions of compound 31 with the PfDHFR-TS protein (Figure 2B) revealed that modifications to its alkyl moiety could significantly enhance the binding affinity of newly designed derivatives by promoting additional interactions with nearby active site residues.

Table 2: Binding energies of Pyrrolone derivatives

S/N	MolDock Score / kcal mol^{-1}	Rerank Score / kcal mol^{-1}	H-Bond / kcal mol^{-1}
1	-146.599	-102.22	-1.844
2	-134.281	-90.672	-1.253
3	-130.211	-93.95	-2.103
4	-133.017	-100.709	-2.486
5	-137.949	-73.106	-4.538
6	-134.189	-82.176	-0.976
7	-138.036	-55.436	-0.397
8	-144.764	-100.727	-1.398
9	-142.626	-46.435	-5.091
10	-142.918	-94.872	-2.088
11	-154.564	-97.773	-0.648
12	-162.968	-113.235	-5.259
13	-156.233	-112.152	-1.897
14	-160.249	-115.988	-2.672
15	-153.419	-107.933	0
16	-156.859	-96.813	-6.974
17	-159.987	-106.276	-1.99
18	-164.276	-111.065	-1.627
19	-158.058	-94.488	-3.954
20	-154.079	-108.64	-4.652
21	-150.299	-110.617	-2.309
22	-154.249	-106.323	-2.5
23	-139.111	-90.824	-4.552
24	-157.647	-78.637	-6.994
25	-150.186	-114.163	-5.436
26	-149.37	-103.799	-1.707
27	-162.644	-73.007	-9.583
28	-154.66	-115.859	-4.601
29	-153.015	-102.405	-2.282
30	-150.738	-110.987	-8.707
31	-167.319	-128.193	-5.418
32	-148.528	-99.855	-4.391
33	-155.992	-111.683	-2.496
34	-151.006	-101.442	-0.422
35	-165.367	-109.497	-6.652
36	-149.854	-118.08	-4.144
37	-155.616	-111.993	-5.129
38	-158.591	-68.228	-5.573

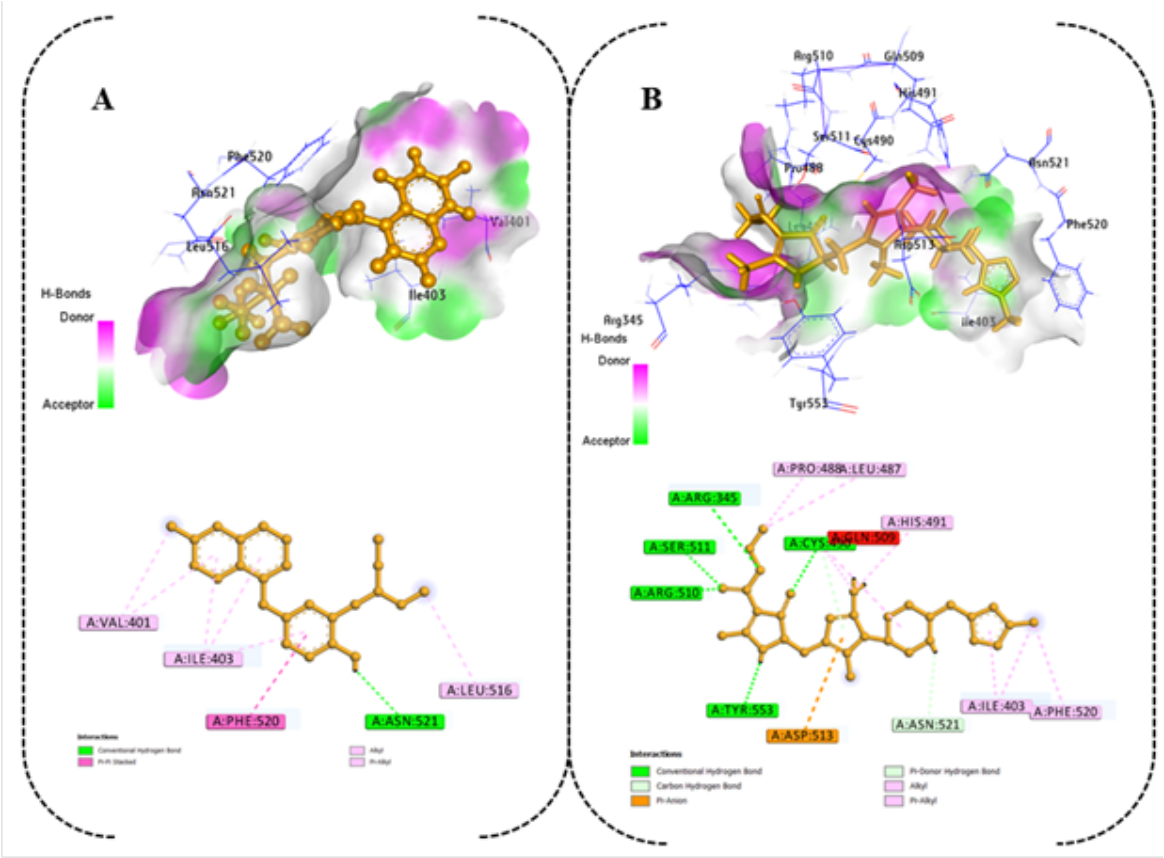

Figure 2: 3-Dimentional and 2-Dimentional interactions of (**A**)- Amodiaquine and (**B**)-Lead compound 31 with PfDHFR-TS receptor (7F3Y).

Functional groups such as nitro (-NO_2), hydroxyl (-OH), alkyl (-CH_2CH_3 and -$C(CH_3)_3$), amine (-NH_2), and halogen (-F) were identified as crucial for improving binding affinity (Table 3) (Abdullahi et al., 2023; Aminu et al., 2022). These functional groups uniquely enhance protein-ligand interactions within the active site by contributing to binding affinity and stability. Polar groups like nitro, hydroxyl, amine, and fluoro are particularly effective in forming hydrogen bonds and dipole-dipole interactions, securing the ligand to specific active site residues (Ja'afaru, et al., 2024). For instance, hydroxyl (-OH) and amine (-NH_2) can serve as both hydrogen bond donors and acceptors, facilitating versatile and robust interactions with polar active amino acid residue (Afagh & Yudin, 2010; Lyu, 2019). Nitro (-NO_2), while limited to hydrogen bond acceptance, provides strong electron-withdrawing effects, stabilizing interactions via resonance and strengthening affinity with charged or polar residues (Olabe, 2020). Meanwhile, nonpolar alkyl groups (-CH_2CH_3 and -$C(CH_3)_3$) contribute significantly to hydrophobic interactions with residues like phenylalanine (-PHE), enhancing the overall stability of the protein-ligand complex. Fluoro (-F), with its strong electron-withdrawing properties, can improve binding through weak hydrogen bonding, favourable interactions with electronegative residues, and enhanced lipophilicity for fitting into hydrophobic pockets. Notably, the addition of these functional groups to the newly designed derivatives enhanced their binding scores (Table 3), suggesting that these modifications could strengthen the derivatives' anti-malaria properties (Table 3). The docking results of the designed compounds (D1-D6) reveal significant improvements in binding affinity, complex stability, and hydrogen bonding interactions compared to both the standard drug Amodiaquine and the lead compound 31 (Table 3). Among the designed derivatives, D5 exhibited the best binding scores, achieving the lowest MolDock score (-172.577 kcal/mol), the most favourable Rerank score (-132.753 kcal/mol), and the strongest hydrogen bond energy (-9.550 kcal/mol). These values indicate superior binding affinity, interaction stability, and hydrogen bonding capacity, making D5 the most promising candidate among the newly designed derivatives. Compared to the lead compound 31 (MolDock score: -163.222 kcal/mol, Rerank score: -69.592 kcal/mol, HBond: -9.644 kcal/mol), most of the designed compounds, particularly D5, D6, and D4, demonstrated enhanced metrics, reflecting their

improved interaction with the target receptor. Moreover, all the designed compounds surpassed the standard drug Amodiaquine (MolDock score: -106.195 kcal/mol, Rerank score: -72.729 kcal/mol, HBond: -3.246 kcal/mol), highlighting the impact of structural modifications on binding efficacy. D5's strong hydrogen bonding interactions and high stability within the active site, as indicated by its binding score energies, suggest that it has the potential to serve as a more effective inhibitor. Overall, the designed compounds, particularly D5, show significant promise as improved drug candidates for targeting the PfDHFR-TS receptor, with their superior docking and binding properties underscoring their potential to outperform existing treatment options. Highlighted in Table 4 are the detailed active-site interactions with the newly designed compounds.

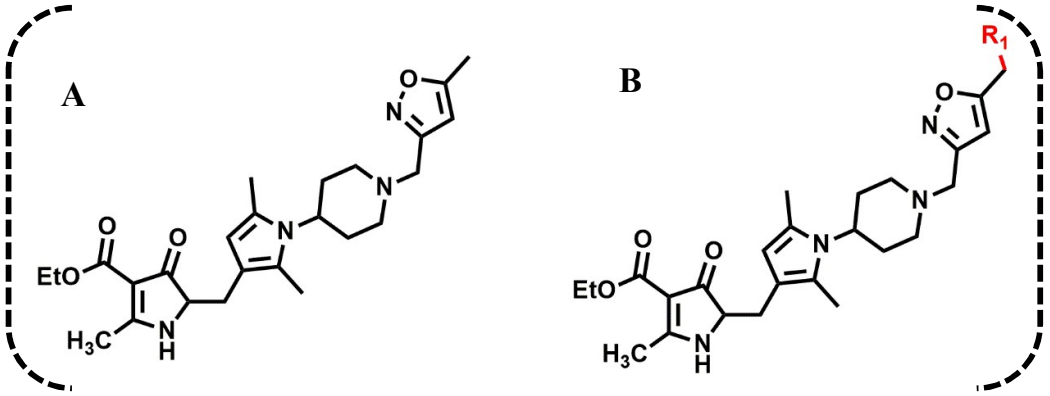

Figure 3: Molecular structures of (**A**)- Compound 31 (Lead) and (**B**)-Design template. R_1 indicates the area of modification.

.

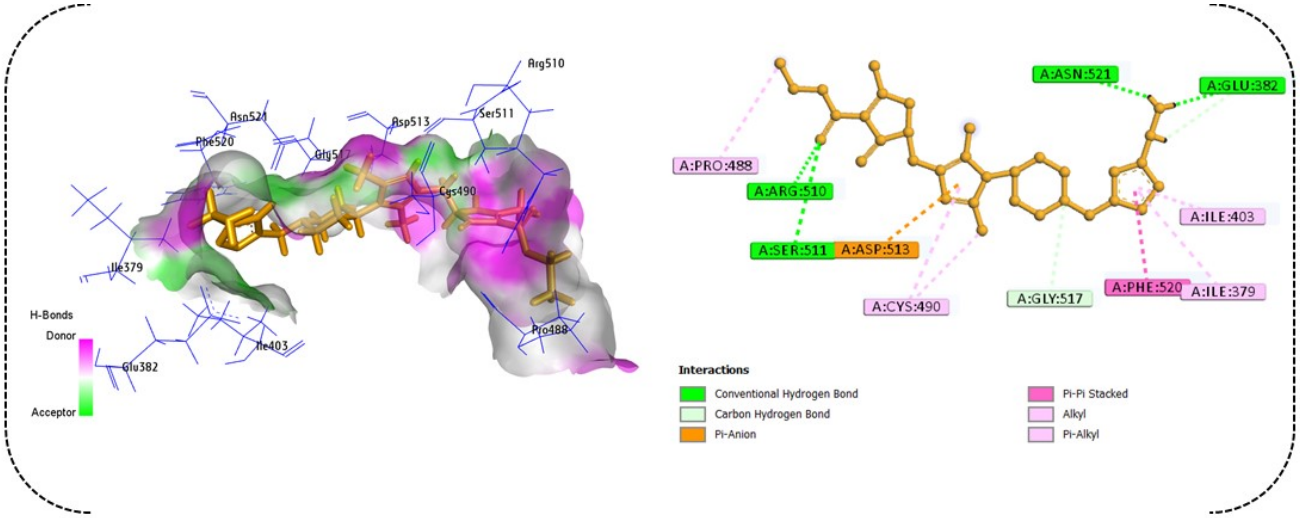

Figure 4: 3-Dimentional and 2-Dimentional interactions of PfDHFR-TS with compound D5

Table 3: Molecular structures, binding energies and Drug score of newly designed Pyrrolone derivatives.

Name	Molecular Structures	MolDock Score / kcal mol^{-1}	Rerank Score / kcal mol^{-1}	H-Bond / kcal mol^{-1}	Drug Score
D1	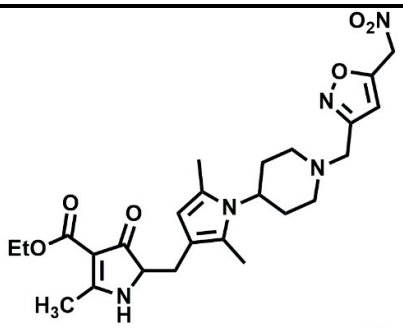	-167.153	-116.459	-7.12205	0.366
D2	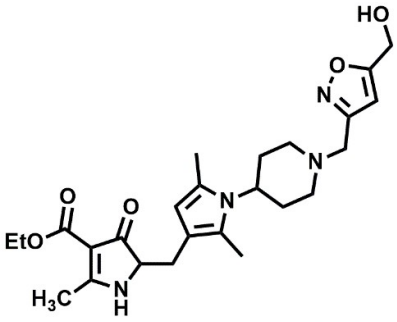	-166.361	-117.234	-8.85746	0.575
D3	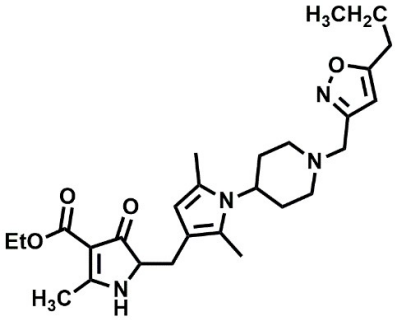	-166.123	-111.167	-3.41829	0.383
D4	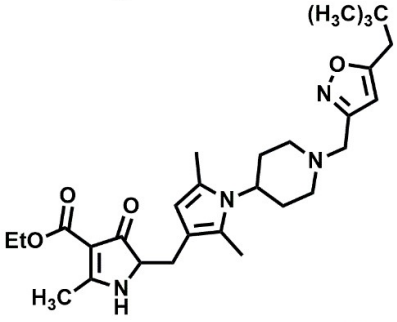	-168.303	-123.666	-8.92665	0.306
D5	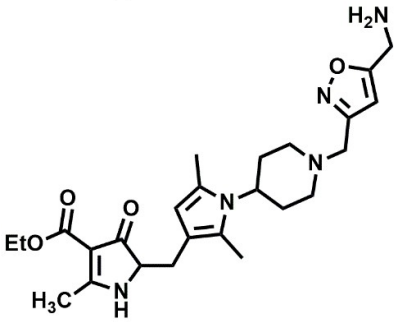	-172.577	-132.753	-9.54998	0.597

D6	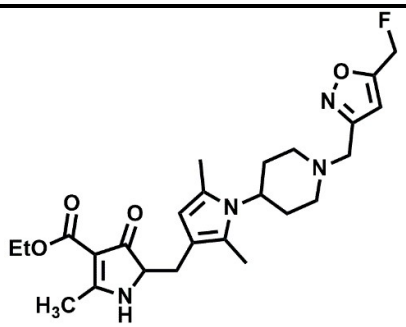	-164.582	-107.339	-3.72754	0.453
31	**Lead compound**	-163.222	-69.5923	-9.6445	0.427
A	**Amodiaquine**	-106.195	-72.7294	-3.24639	0.137

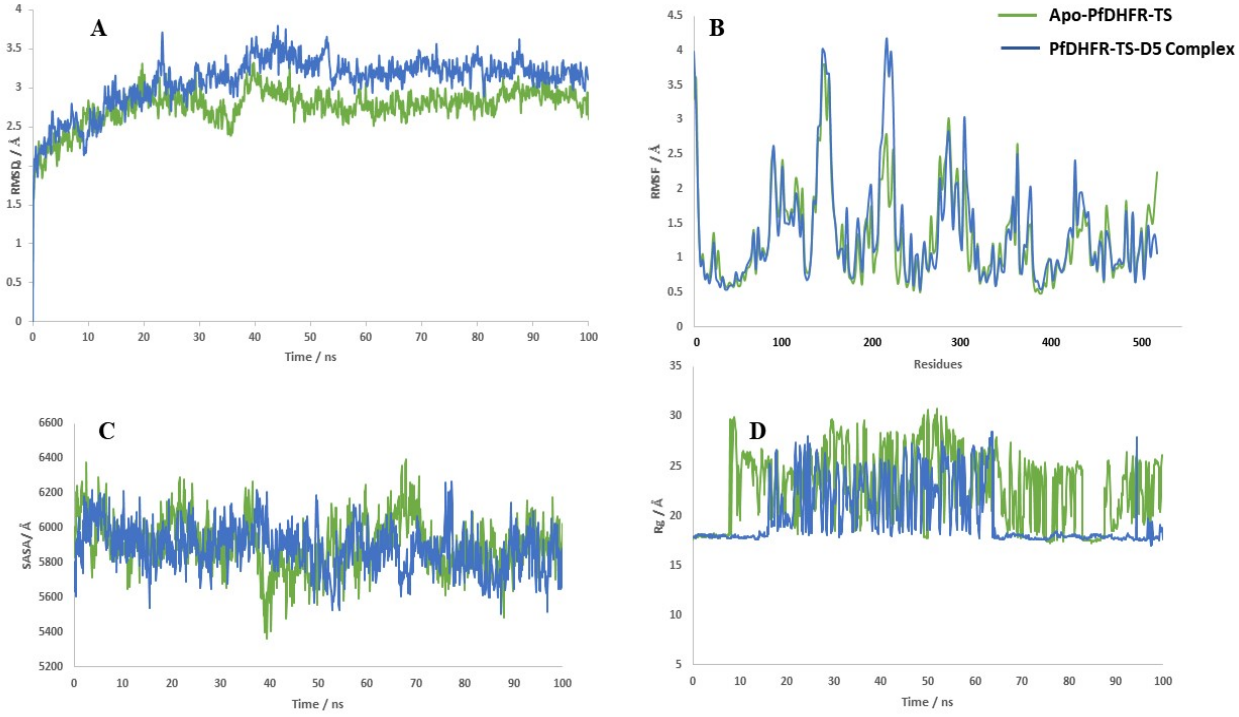

Figure 5: 100 ns molecular dynamics simulation analysis of PfDHFR-TS apo protein and PfDHFR-TS-D5 complex, (A)- RMSD plot, (B)-RMSF plot, (C)-SASA plot and (D)-Rg plot.

The protein-ligand interaction data provided in Table 4 demonstrates a series of significant hydrogen bonds critical for stabilizing the designed compounds in the active site. Key residues involved in these interactions include, ARG510, ARG377, HIS551, SER511, GLY378, ARG402, ILE403, and CYS490. Among these, the best designed compounds (**D5**) shows four conventional hydrogen bonding interactions particularly with ARG510, SER511, ASN521 and GLU382 with a short interaction distance of 1.624 Å, 2.843 Å, 2.239 Å and 2.181 Å, likely acting as a key anchor for ligand stability. Similarly, GLY517 and GLU382 show strong carbon-hydrogen interactions at distances of 2.405 Å and 3.058 Å, respectively, further supporting ligand alignment and orientation (Table 4, Figure 4). Moreover, several hydrophobic interactions were identified between the ligand **D5** and key active site residues of the PfDHFR-TS receptor, including ASP513, PHE520, PRO488, CYS490, ILE379, and ILE403. Importantly, all six designed compounds exhibit significant hydrogen bonding interactions, with bond distances falling within the optimal range, contributing to strong stabilization within the binding pocket. This network of conventional hydrogen bonds highlights the compounds' potential for high-

affinity binding, emphasizing their importance in enhancing the therapeutic efficacy of the designed molecules.

Molecular dynamics simulation

The molecular dynamics (MD) simulation analysis of the apo-PfDHFR-TS and the PfDHFR-TS-**D5** complex provides important information about their structural dynamics and stability under physiological conditions (Kumari, et al., 2017). The root-mean-square deviation (RMSD) analysis over a 100 ns molecular dynamics (MD) simulation reveals distinct stability patterns for the apo-PfDHFR-TS and the PfDHFR-TS-D5 complex (Figure 5A). Both systems show an initial RMSD increase within the first 25 ns, indicating structural adjustments as the systems equilibrate. The apo-PfDHFR-TS stabilizes thereafter, maintaining RMSD values between 2.5 and 3.0 Å, suggesting a relatively stable protein structure throughout the simulation. In contrast, the PfDHFR-TS-D5 complex stabilizes at slightly higher RMSD values of 3.0 to 3.5 Å from 25 ns onward, reflecting the additional conformational adjustments required to accommodate the D5 ligand
.

Table 4: PfDHFR-TS receptor active site amino-acid residue interactions with newly designed compounds

Complex	Active amino acid residue	Interaction Distance	Category of interaction	Type of interaction
D1	ARG377	2.999	Hydrogen Bond	Conventional Hydrogen Bond
	GLY378	2.841	Hydrogen Bond	Conventional Hydrogen Bond
	ARG402	1.773	Hydrogen Bond	Conventional Hydrogen Bond
	ILE403	2.753	Hydrogen Bond	Conventional Hydrogen Bond
	CYS490	2.318	Hydrogen Bond	Conventional Hydrogen Bond
	ASN521	2.316	Hydrogen Bond	Conventional Hydrogen Bond
	VAL401	3.044	Hydrogen Bond	Carbon Hydrogen Bond
	ILE403	4.058	Hydrophobic	Alkyl
	ILE379	4.948	Hydrophobic	Alkyl
	PHE520	5.354	Hydrophobic	Pi-Alkyl
	ILE403	5.488	Hydrophobic	Pi-Alkyl
	VAL401	5.385	Hydrophobic	Pi-Alkyl
	ARG402	4.973	Hydrophobic	Pi-Alkyl
D2	ILE379	2.251	Hydrogen Bond	Conventional Hydrogen Bond
	CYS490	1.724	Hydrogen Bond	Conventional Hydrogen Bond
	ASN521	2.169	Hydrogen Bond	Conventional Hydrogen Bond
	PHE375	1.586	Hydrogen Bond	Conventional Hydrogen Bond
	PHE375	2.993	Hydrogen Bond	Carbon Hydrogen Bond
	PHE520	4.07	Hydrophobic	Pi-Pi Stacked
	ILE403	5.163	Hydrophobic	Alkyl
	LEU516	5.185	Hydrophobic	Alkyl
	LEU516	4.763	Hydrophobic	Alkyl
	ILE403	4.537	Hydrophobic	Pi-Alkyl
D3	TYR553	2.459	Hydrogen Bond	Conventional Hydrogen Bond
	GLY517	2.26	Hydrogen Bond	Carbon Hydrogen Bond
	ARG345	3.114	Hydrogen Bond	Pi-Donor Hydrogen Bond
	CYS490	5.545	Other	Pi-Sulfur
	CYS490	4.403	Hydrophobic	Alkyl
	CYS490	3.74	Hydrophobic	Alkyl
	TYR430	5.302	Hydrophobic	Pi-Alkyl
	HIS491	4.317	Hydrophobic	Pi-Alkyl
	HIS491	4.944	Hydrophobic	Pi-Alkyl
	HIS551	3.997	Hydrophobic	Pi-Alkyl
	ARG345	4.74	Hydrophobic	Pi-Alkyl

D4	CYS490	2.669	Hydrogen Bond	Conventional Hydrogen Bond
	ARG510	1.849	Hydrogen Bond	Conventional Hydrogen Bond
	SER511	2.113	Hydrogen Bond	Conventional Hydrogen Bond
	ASN521	1.854	Hydrogen Bond	Carbon Hydrogen Bond
	GLU382	2.982	Hydrogen Bond	Carbon Hydrogen Bond
	ASP513	4.582	Electrostatic	Pi-Anion
	CYS490	4.218	Other	Pi-Sulfur
	CYS490	5.127	Hydrophobic	Alkyl
	LEU487	3.641	Hydrophobic	Alkyl
	PRO488	4.038	Hydrophobic	Alkyl
	CYS490	4.304	Hydrophobic	Alkyl
	LEU516	4.926	Hydrophobic	Alkyl
	PHE520	4.694	Hydrophobic	Pi-Alkyl
	ILE403	4.071	Hydrophobic	Pi-Alkyl
D5	ARG510	1.624	Hydrogen Bond	Conventional Hydrogen Bond
	SER511	2.843	Hydrogen Bond	Conventional Hydrogen Bond
	ASN521	2.239	Hydrogen Bond	Conventional Hydrogen Bond
	GLU382	2.181	Hydrogen Bond	Conventional Hydrogen Bond
	GLY517	2.405	Hydrogen Bond	Carbon Hydrogen Bond
	GLU382	3.058	Hydrogen Bond	Carbon Hydrogen Bond
	ASP513	4.478	Electrostatic	Pi-Anion
	PHE520	4.663	Hydrophobic	Pi-Pi Stacked
	PRO488	3.873	Hydrophobic	Alkyl
	CYS490	4.292	Hydrophobic	Alkyl
	CYS490	4.767	Hydrophobic	Pi-Alkyl
	ILE379	5.318	Hydrophobic	Pi-Alkyl
	ILE403	4.676	Hydrophobic	Pi-Alkyl
D6	ARG345	2.886	Hydrogen Bond; Halogen	Conventional Hydrogen Bond; Halogen (Fluorine)
	ASN407	2.851	Hydrogen Bond	Conventional Hydrogen Bond
	GLU382	2.391	Hydrogen Bond	Carbon Hydrogen Bond
	ASP513	2.349	Hydrogen Bond	Carbon Hydrogen Bond
	SER511	2.874	Hydrogen Bond	Carbon Hydrogen Bond
	TYR553	2.539	Hydrogen Bond	Carbon Hydrogen Bond
	ARG345	4.495	Electrostatic	Pi-Cation
	CYS490	5.86	Other	Pi-Sulfur
	CYS490	5.118	Other	Pi-Sulfur
	SER511	2.994	Other	Pi-Lone Pair
	CYS490	4.983	Hydrophobic	Alkyl
	LEU487	4.408	Hydrophobic	Alkyl
	CYS490	3.221	Hydrophobic	Alkyl
	ARG345	3.823	Hydrophobic	Alkyl
	HIS491	4.115	Hydrophobic	Pi-Alkyl

This higher RMSD in the complex likely represents the dynamic interactions between the protein and ligand, while still indicating overall system stability (Liu, et al., 2017). The root-mean-square fluctuation (RMSF) analysis over the 100 ns simulation period reveals a similar pattern of flexibility for both the apo-PfDHFR-TS and the PfDHFR-TS-D5 complex, with some subtle differences (Figure 5B). Both systems exhibit stable RMSF profiles throughout the simulation, indicating relatively consistent structural behaviour. However, the PfDHFR

-TS-**D5** complex shows slightly higher RMSF values between residues 200 to 240, suggesting that this region becomes more flexible upon ligand binding. This increased flexibility may reflect the dynamic interactions between the ligand and the protein, particularly in regions that may be involved in ligand recognition or binding site fluctuation. In contrast, the apo-PfDHFR-TS maintains a more rigid conformation in this region, further reinforcing the idea that ligand binding triggers localized conformational changes, enabling better interaction with the receptor (Du, et al., 2024). Additionally, a Solvent Accessible Surface Area (SASA) plot provides insights into the protein's surface exposure to the solvent over time. It helps assess the protein's compactness and conformational changes**,** with decreased SASA indicating a more folded or stable structure, and increased SASA suggesting a more extended or flexible state Raghunathan, 2024; Saini & Kumar, 2024). The SASA plot from the 100 ns simulation period shows slightly higher values for the apo-PfDHFR-TS throughout the simulation, suggesting that this protein is more exposed to the solvent, likely due to a more open or less compact structure in the absence of the ligand. In contrast, the PfDHFR-TS-**D5** complex exhibits lower SASA values, indicating that the binding of the **D5** ligand stabilizes the protein, leading to a more compact conformation with reduced solvent exposure (Figure 5C). Regarding the radius of gyration (Rg) plot, the PfDHFR-TS-**D5** complex maintains a steady Rg value of about 17.5 Å from 0 to 17 ns, indicating a stable, compact structure. Between 20 to 65 ns, the Rg fluctuates slightly between 17.5 to 25 Å, suggesting some internal motions but overall maintaining stability. After 65 ns, the Rg becomes steady again around 18 Å, reinforcing the ligand-bound structure's compactness and stability. On the other hand, the apo-PfDHFR-TS shows constant fluctuations in Rg, ranging from 18 to 30 Å throughout the simulation. This larger fluctuation suggests that the apoprotein is more flexible and undergoes larger conformational changes due to the absence of a stabilizing ligand. Notably, these results indicate that the binding of the **D5** ligand to PfDHFR-TS leads to a more compact and stable protein structure, whereas the apoprotein remains more dynamic and flexible, which may impact its functional stability.

Drug-likeness Analysis

The drug score results of the designed compounds (**D1-D6**) were calculated to evaluate their overall drug-like properties, including factors such as molecular weight, lipophilicity, hydrogen bond donors and acceptors, and other pharmacokinetic characteristics (Mukadam & Jagdale). These drug scores provide an understanding of the potential of the compounds to be developed as viable drugs. Among the designed compounds, **D5** consistently outperformed the others with the highest drug score of 0.597, signalling its favourable drug-like properties (Table 3). It exhibited a more balanced profile in terms of molecular characteristics, suggesting it has better pharmacokinetic potential for oral bioavailability and permeability. Compounds **D2** and **D6** followed closely, with good drug scores, indicating that these compounds also hold strong potential for further development. The drug scores of compounds **D1**, **D3**, and **D4**, while still promising, were slightly lower, which may indicate slight drawbacks in terms of their molecular properties, such as higher molecular weight or undesirable lipophilicity, which could affect their pharmacokinetics. Notably, when compared to the standard drug Amodiaquine, which had a drug score that was relatively lower (0.137), the designed compounds generally showed better potential. Amodiaquine, though effective in its use, showed suboptimal properties in terms of lipophilicity and other pharmacokinetic factors, which is why the designed compounds could present improvements in bioavailability and efficacy. The lead compound **31**, while exhibiting a good drug score (0.427) still lagged behind **D5** in terms of its overall drug-like properties. This suggests that, although compound **31** shows strong binding affinity, modifications in the designed compounds (such as in **D5**) have led to enhanced pharmacokinetic profiles, making these derivatives more favourable as potential drug candidates

Table 5: ADMET Parameters of Newly Designed Derivatives

Name	I/A (Human)	BBB	CNS	CYP34A		T-Clearance	AMES Toxic
				Substrate	Inhibitor		
D1	80.633	-1.315	-3.155	Yes	Yes	0.729	No
D2	74.847	-1.129	-3.155	Yes	Yes	1.064	No
D3	94.851	-0.824	-2.981	Yes	Yes	1.132	No
D4	93.107	-0.741	-2.885	Yes	Yes	0.765	No
D5	76.480	-1.034	-3.139	Yes	No	1.085	No
D1	80.633	-1.315	-3.155	Yes	Yes	0.729	No

***Key**: I/A (Human)- Human Intestinal absorption (% Absorbed); BBB- Blood brain barrier permeability (Log BB); CNS- Central nervous system permeability (log PS).*

ADMET-predictions

The six novel anti-malaria compounds exhibit promising pharmacokinetic and toxicity profiles, making them strong candidates for further development. All compounds demonstrate high intestinal absorption, with an average of 85.85% and a range of 74.85% to 95.21%, suggesting excellent potential for oral administration. The CNS-targeting drugs as it reduces the risk of central nervous system side effects. Similarly, their low CNS penetration scores (mean: -3.06) confirm limited CNS accessibility. This aligns well with the therapeutic goal of targeting malaria outside the CNS. Metabolically, all compounds act as substrates and inhibitors of CYP3A4, a critical enzyme in drug metabolism, raising concerns about potential drug-drug interactions (Zhou, 2008). The total clearance values range from 0.73 to 1.13 (mean: 0.97), suggesting moderate to low systemic clearance, which may lead to prolonged half-lives and less frequent dosing. However, compounds with lower clearance, such as **D1** (0.73), need to be evaluated for potential accumulation and associated toxicity. Importantly, all compounds are non-mutagenic, as shown by the Ames test, highlighting their safety regarding genetic toxicity (da Silva, et al., 2020). The consistent absorption, distribution, and metabolic behaviour across the compounds indicate a shared chemical framework, simplifying safety predictions. Moving forward, *in vitro* and *in vivo* studies are recommended to confirm CYP3A4 interactions and evaluate other metabolic pathways.

Density Functional Theory (DFT) Analysis

The density functional theory (DFT) study was performed to investigate the electronic properties of the compounds in detail, as these characteristics significantly impact the molecules' binding affinity to the target protein (Hagar, et al., 2020). The highest occupied molecular orbital (HOMO) and lowest unoccupied molecular orbital (LUMO) define the compounds' donor-acceptor capabilities, which are essential for electronic interactions within the active site. The band gap energy ($\Delta E_{(HOMO-LUMO)}$) provides insights into the compounds' overall stability and reactivity, while the electrostatic potential maps reveal specific regions of the molecules prone to interactions like hydrogen bonding or ionic interactions (Mumit et al., 2020). Additionally, the density of states (DOS) analysis offers a deeper understanding of the distribution of electronic states and their role in molecular interactions (Fung et al., 2021). This research employed DFT calculations using the B3LYP functional and 6-31G* basis set to examine the electronic properties of the design template, Compound **31**, and the newly designed compound, **D5**. The study focuses on the HOMO and LUMO energies, band gap ($\Delta E_{(HOMO-LUMO)}$), electrostatic potential maps, and DOS to shed light on the compounds' electronic characteristics and their significance in binding interactions with the target protein, PfDHFR-TS (Figure 6).

Band Gap Analysis

The band gap energy signifies the difference in energy between the HOMO and LUMO orbitals and is a crucial factor in determining the chemical reactivity and stability of the compounds (Sevvanthi et al., 2020). From the generated plots, Compound **31** has a band gap energy of -4.12 eV, while **D5** exhibits a slightly larger band gap energy of -4.17 eV (Figure 6A and 6B). This marginal increase in the band gap suggests that compound **D5** is slightly more stable but still retains sufficient reactivity for strong interactions with the target protein. The small variation in the band gap may reflect subtle changes in electronic distribution due to the introduction of the $-NH_2$ substituent in the designed compound (**D5**).

Electrostatic Potential Map

The electrostatic potential (ESP) map visually depicts the charge distribution across the molecular surface, offering an understanding of how the compound interacts with the electrostatic environment of the protein's active site (Rathi et al., 2019). For compound **D5**, the ESP map reveals an additional electro-rich region near the $-NH_2$ substituent, which is not present in Compound **31** (Figures 6C and 6D). This electronegative region facilitates stronger hydrogen bond interactions between **D5** and the active site amino acid residues ASN521 and GLU382, thereby enhancing its binding affinity.

Density of States (DOS) Analysis

The DOS plots for the two compounds reveal slight differences in electronic distribution around the Fermi level (Figures 6C and 6D. In **D5**, the additional $-NH_2$ group influences the electron density, potentially redistributing electronic states near the HOMO and LUMO energy levels. This redistribution enhances the compound's ability to engage in π-stacking interactions with the target protein specifically with PHE520 residue. The changes observed in the DOS suggest that the electronic environment of **D5** is better optimized for interaction with the active site compared to that of Compound **31**.

Conclusion

In conclusion, this *in-silico* study introduces a set of newly designed compounds (**D1-D6**) as promising inhibitors of *Plasmodium falciparum* dihydrofolate reductase-thymidylate synthase (PfDHFR-TS). The molecular docking scores

of these compounds surpassed those of both the template (**31)** compound and the standard drug, Amodiaquine. Notably, compound **D5** demonstrated strong binding stability with the active amino acid residues in the PfDHFR-TS binding site, as confirmed by a 100 ns molecular dynamics simulation. Additionally, the designed compounds exhibited favourable drug-like properties, good pharmacokinetics, and favourable DFT parameters. These findings support the need for further synthesis and experimental validation of the proposed compounds as potential PfDHFR-TS inhibitors for the treatment of malaria.

Acknowledgement

The authors wish to express their sincere gratitude to TETFUND (Tertiary Education Trust Fund) for the generous financial support provided through the grant awarded to Jigawa State Polytechnic. This funding has been instrumental in facilitating the execution of this project, enabling us to undertake our research and achieve our objectives effectively.

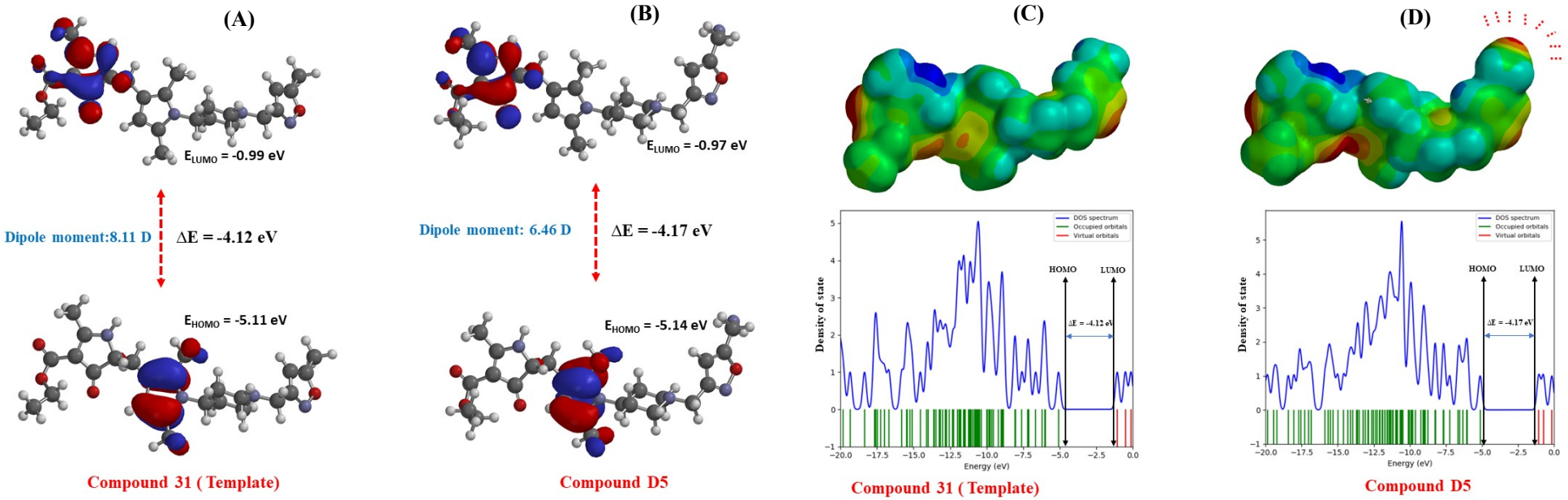

Figure 6: density functional theory analysis of the lead compound (**31**) and the best designed compound (D5). (**A**)-HOMO-LUMO orbitals of compound **31;** (**B**) -HOMO-LUMO orbitals of compound **31 (C**)-Electro-potential map of compound **31**: and (**D**))-Electro-potential map of compound **D5.**

References

Abdullahi SH, Moin AT, Uzairu A, Umar AB, Ibrahim MT, Usman MT, Nawal N, Bayil I, Zubair T: Molecular docking studies of some benzoxazole and benzothiazole derivatives as VEGFR-2 target inhibitors: In silico design, MD simulation, pharmacokinetics and DFT studies. Intelligent Pharmacy 2023.

Abdullahi SH, Uzairu A, Shallangwa GA, Uba S, Umar AB: Pharmacokinetic profiling of quinazoline-4(3H)-one analogs as EGFR inhibitors: 3D-QSAR modeling, molecular docking studies and the design of therapeutic agents. Journal of Taibah University Medical Sciences 2023, 18(5):1018-1029.

Afagh NA, Yudin AK: Chemoselectivity and the curious reactivity preferences of functional groups. Angewandte Chemie International Edition 2010, 49(2):262-310.

Alghamdi, J. M., Al-Qahtani, A. A., Alhamlan, F. S., & Al-Qahtani, A. A. (2024). Recent advances in the treatment of malaria. *Pharmaceutics, 16*(11), 1416.

Ameji, J. P., Uzairu, A., Shallangwa, G. A., & Uba, S. I. (2024). Theoretical investigation and design of bioactive quinoline derivatives as inhibitors of DNA gyrase of *Salmonella typhi*. *Malaysian Journal of Pharmaceutical Sciences, 22*(1), 1-20.

Aminu KS, Uzairu A, Umar AB, Ibrahim MT: Salicylic acid derivatives as potential α-glucosidase inhibitors: drug design, molecular docking and pharmacokinetic studies. Bulletin of the National Research Centre 2022, 46(1):162.

Azzam, K. A. (2023). SwissADME and pkCSM webservers predictors: An integrated online platform for accurate and comprehensive predictions for in silico ADME/T properties of artemisinin and its derivatives. *Kompleksnoe Ispolzovanie Mineralnogo Syra= Complex Use of Mineral Resources, 325*(2), 14-21.

Bassani, D., & Moro, S. (2023). Past, present, and future perspectives on computer-aided drug design methodologies. *Molecules, 28*(9), 3906.

Bharatam, P. V. (2021). Computer-aided drug design. In *Drug Discovery and Development: From Targets and Molecules to Medicines* (pp. 137-210).

da Fonseca, A. M., Caluaco, B. J., Madureira, J. M. C., Cabongo, S. Q., Gaieta, E. M., Djata, F., Colares, R. P., Neto, M. M., Fernandes, C. F. C., & Marinho, G. S. (2024). Screening of potential inhibitors targeting the main protease structure of SARS-CoV-2 via molecular docking, and approach with molecular dynamics, RMSD, RMSF, H-bond, SASA, and MMGBSA. *Molecular Biotechnology, 66*(8), 1919-1933.

da Silva Dantas FG, de Castilho PF, de Almeida-Apolonio AA, de Araújo RP, de Oliveira KMP: Mutagenic potential of medicinal plants evaluated by the Ames Salmonella/microsome assay: A systematic review. Mutation Research/Reviews in Mutation Research 2020, 786:108338.

Du R, Li L, Ji J, Fan Y: Receptor–Ligand Binding: Effect of Mechanical Factors. Int J Mol Sci 2023, 24(10):9062.

Fischer, A., Smiesko, M., Sellner, M., & Lill, M. A. (2021). Decision making in structure-based drug discovery: Visual inspection of docking results. *Journal of Medicinal Chemistry, 64*(5), 2489-2500.

Fung V, Hu G, Ganesh P, Sumpter BG: Machine learned features from density of states for accurate adsorption energy prediction. Nature communications 2021, 12(1):88.

Garrido-Cardenas, J. A., González-Cerón, L., García-Maroto, F., Cebrián-Carmona, J., Manzano-Agugliaro, F., & Mesa-Valle, C. M. (2023). Analysis of fifty years of severe malaria worldwide research. *Pathogens, 12*(3), 373.

Guin M, Halder S, Chatterjee S, Konar S: Synthesis, X-ray crystal structure of Cu (II) 1D coordination Polymer: In View of Hirshfeld surface, FMO, Molecular electrostatic potential (MEP) and Natural Bond orbital (NBO) analyses. Journal of molecular structure 2022, 1270:133949.

Hagar M, Ahmed HA, Aljohani G, Alhaddad OA: Investigation of some antiviral N-heterocycles as COVID 19 drug: molecular docking and DFT calculations. Int J Mol Sci 2020, 21(11):3922.

Hassan, E. M., Mustafa, Y. F., & Merkhan, M. M. (2022). Computation in chemistry: Representative software and resources. *Int J Pharmacy Pharm St, 6*(2), 1-10.

Ja'afaru SC, Uzairu A, Sallau MS, Ndukwe GI, Ibrahim MT, Danazumi AU: Structure-Based Design of Potential Anti-schistosomiasis Agent Targeting SmHDAC8: An In Silico Approach Utilizing QSAR, MD Simulation and ADMET Prediction. Chemistry Africa 2023:1-21.

Ja'afaru SC, Uzairu A, Chandra A, Sallau MS, Ndukwe GI, Ibrahim MT, Qamar I: Ligand based-design of potential schistosomiasis inhibitors through QSAR, homology modeling, molecular dynamics, pharmacokinetics, and DFT studies. Journal of Taibah University Medical Sciences 2024, 19(2):429-446.

Jáafaru, S. C., Uzairu, A., Sallau, M. S., Ndukwe, G. I., Ibrahim, M. T., Tabti, K., Kandpal, P., & Kumar, V. (2024). In-silico exploration and structure-based design of praziquantel derivatives as potential inhibitors of *Schistosoma mansoni* glutathione S-transferase (SmGST). *Scientific African, e02169*.

Khelfa, N. (2024). Virtual screening applied in several series of bioactive heterocyclic molecules. *Université Mohamed Khider (Biskra-Algérie)*.

Khurshid, F. (2024). Computer simulation of simple and complex electrolyte solutions. *Kansas State University*.

Kogan, F., & Kogan, F. (2020). Malaria burden. In *Remote Sensing for Malaria: Monitoring and Predicting Malaria from Operational Satellites* (pp. 15-41).

Kolawole, E. O., Ayeni, E. T., Abolade, S. A., Ugwu, S. E., Awoyinka, T. B., Ofeh, A. S., & Okolo, B. O. (2023). Malaria endemicity in Sub-Saharan Africa: Past and present issues in public health. *Microbes and Infectious Diseases, 4*(1), 242-251.

Kumari I, Sandhu P, Ahmed M, Akhter Y: Molecular dynamics simulations, challenges and opportunities: a Biologist's prospective. Current Protein and Peptide Science 2017, 18(11):1163-1179.

Lartey, S. (n.d.). Exploring the impact of malaria on global health: Financial implications and strategies for prevention.

Li, B., Wang, Z., Liu, Z., Tao, Y., Sha, C., He, M., & Li, X. (2024). DrugMetric: Quantitative drug-likeness scoring based on chemical space distance. *Briefings in Bioinformatics, 25*(4), bbae321.

Liu K, Watanabe E, Kokubo H: Exploring the stability of ligand binding modes to proteins by molecular dynamics simulations. Journal of computer-aided molecular design 2017, 31:201-211.

Loh, Z. N. (2023). Nuclear PTEN regulates thymidylate biosynthesis and cellular sensitivity to antifolate treatment. *Duke University*.

Lyu Y: The interaction of biomolecules with gold nanoparticles: from amine-driven binding to covalent capture. 2019.

Marttila, P. (2023). Targeting MTHFD1 and MTHFD2 as cancer treatment. *Karolinska Institutet (Sweden)*.

Maurya, V. K., Kumar, S., Prasad, A. K., Bhatt, M. L., & Saxena, S. K. (2020). Structure-based drug designing for potential antiviral activity of selected natural products from Ayurveda against SARS-CoV-2 spike glycoprotein and its cellular receptor. *Virusdisease, 31*, 179-193.

Mukadam, M. M., & Jagdale, D. M. (2024). In silico ADME/T prediction of steroidal chalcone derivatives using Swiss ADME and OSIRIS explorer. *Research Journal of Pharmacy and Technology, 17*(2), 843-848.

Mumit MA, Pal TK, Alam MA-A-A-A, Islam MA-A-A-A, Paul S, Sheikh MC: DFT studies on vibrational and electronic spectra, HOMO–LUMO, MEP, HOMA, NBO and molecular docking analysis of benzyl-3-N-(2, 4, 5-trimethoxyphenylmethylene) hydrazinecarbodithioate. Journal of molecular structure 2020, 1220:128715.

Murugesan, D., Kaiser, M., White, K. L., Norval, S., Riley, J., Wyatt, P. G., Charman, S. A., Read, K. D., Yeates, C., & Gilbert, I. H. (2013). Structure-activity relationship studies of pyrrolone antimalarial agents. *ChemMedChem, 8*(9), 1537-1544.

Nascimento, I. J. d. S., de Aquino, T. M., & da Silva-Júnior, E. F. (2022). The new era of drug discovery: The power of computer-aided drug design (CADD). *Letters in Drug Design & Discovery, 19*(11), 951-955.

Nuga, O. A., Adigun, A. J., Emmanuel, O. S., & Abdulhamid, A. Z. (2024). A machine learning model for assessing the prevalence of counterfeit antimalarial in geographical zones of Nigeria. *International Journal of Innovative Research in Medical Science (IJIRMS), 9*(05).

Obeagu, E. I., & Obeagu, G. U. (2024). Emerging public health strategies in malaria control: Innovations and implications. *Annals of Medicine and Surgery, 86*(11), 6576-6584.

Obeagu, E., & Obeagu, G. (2024). Overcoming hurdles: Anemia management in malaria-affected childhood. *Elite Journal of Laboratory Medicine, 2*(1), 59-69.

Ojha, P. K., Kumar, V., Roy, J., & Roy, K. (2021). Recent advances in quantitative structure–activity relationship models of antimalarial drugs. *Expert Opinion on Drug Discovery, 16*(6), 659-695.

Okumu, F., Gyapong, M., Casamitjana, N., Castro, M. C., Itoe, M. A., Okonofua, F., & Tanner, M. (2022). What Africa can do to accelerate and sustain progress against malaria. *PLOS Global Public Health, 2*(6), e0000262.

Olabe J: Coordination chemistry of nitric oxide and biological signaling. Science Reviews-from the end of the world 2020, 2(1):64-99.

Oladoyinbo, O. B. (2018). Influence of malaria incidences on lifestyle and farming activities of rice farmers in South-West, Nigeria.

Olaoye, F., Potter, K., & Egon, A. (2024). Protein-ligand interactions and drug design. *Med Chem*.

Oluyemi, W. M., Nwokebu, G., Adewumi, A. T., Eze, S. C., Mbachu, C. C., Ogueli, E. C., Nwodo, N., Soliman, M. E., Mosebi, S. (2024). The characteristic structural and functional dynamics of *P. falciparum* DHFR binding with pyrimidine chemotypes implicate malaria therapy design. *Chemical Physics Impact, 9*, 100703.

Prasad, K., Nikzad, M., Nisha, S. S., & Sbarski, I. (2021). On the use of molecular dynamics simulations for elucidating fine structural, physico-chemical and thermomechanical properties of lignocellulosic systems:

Historical and future perspectives. *Journal of Composites Science, 5*(2), 55.

Raghunathan S: Solvent accessible surface area-assessed molecular basis of osmolyte-induced protein stability. RSC advances 2024, 14(34):25031-25041.

Rathi PC, Ludlow RF, Verdonk ML: Practical high-quality electrostatic potential surfaces for drug discovery using a graph-convolutional deep neural network. Journal of medicinal chemistry 2019, 63(16):8778-8790.

Rong C, Wang B, Zhao D, Liu S: Information-theoretic approach in density functional theory and its recent applications to chemical problems. Wiley Interdisciplinary Reviews: Computational Molecular Science 2020, 10(4):e1461.

Saini S, Kumar Y: Structural and functional analysis of engineered antibodies for cancer immunotherapy: insights into protein compactness and solvent accessibility. Journal of Biomolecular Structure and Dynamics 2023:1-14.

Sert, Y., Lahmidi, S., El Hafi, M., Gökce, H., Essassi, E. M., Ejjoumamany, A., & Mague, J. T. (2020). Spectral, DFT/B3LYP and molecular docking analyses on ethyl 2-(5-methyl-1, 2, 4-triazolo [1, 5-a] pyrimidin-7-yl) pent-4-enoate. *Journal of Molecular Structure, 1206*, 127680.

Sevvanthi S, Muthu S, Aayisha S, Ramesh P, Raja M: Spectroscopic (FT-IR, FT-Raman and UV-Vis), computational (ELF, LOL, NBO, HOMO-LUMO, Fukui, MEP) studies and molecular docking on benzodiazepine derivatives-heterocyclic organic arenes. Chemical Data Collections 2020, 30:100574.

Shah, V. R., Bhaliya, J. D., & Patel, G. M. (2021). In silico approach: Docking study of oxindole derivatives against the main protease of COVID-19 and its comparison with existing therapeutic agents. *Journal of Basic and Clinical Physiology and Pharmacology, 32*(3), 197-214.

Shamshad, H., Bakri, R., & Mirza, A. Z. (2022). Dihydrofolate reductase, thymidylate synthase, and serine hydroxy methyltransferase: Successful targets against some infectious diseases. *Molecular Biology Reports, 49*(7), 6659-6691.

Shivanika C, Kumar D, Ragunathan V, Tiwari P, Sumitha A: Molecular docking, validation, dynamics simulations, and pharmacokinetic prediction of natural compounds against the SARS-CoV-2 main-protease. Journal of biomolecular structure & dynamics 2020:1.

Smardz, P., Anila, M., Rogowski, P., Li, M., Rózycki, B., & Krupa, P. (2024). A practical guide to all-atom and coarse-grained molecular dynamics simulations using Amber and Gromacs: A case study of disulfide-bond impact on the intrinsically disordered amyloid beta. *Int J Mol Sci, 25*, 6698.

Talapko, J., Škrlec, I., Alebić, T., Jukić, M., & Včev, A. (2019). Malaria: The past and the present. *Microorganisms, 7*(6), 179.

Tanramluk D, Pakotiprapha D, Phoochaijaroen S, Chantravisut P, Thampradid S, Vanichtanankul J, Narupiyakul L, Akavipat R, Yuvaniyama J: MANORAA: A machine learning platform to guide protein-ligand design by anchors and influential distances. Structure (London, England : 1993) 2022, 30(1):181-189.e185.

Thomsen, R., & Christensen, M. H. (2006). MolDock: A new technique for high-accuracy molecular docking. *Journal of Medicinal Chemistry, 49*(11), 3315-3321.

Tiwari, P. C., Pal, R., Chaudhary, M. J., & Nath, R. (2023). Artificial intelligence revolutionizing drug development: Exploring opportunities and challenges. *Drug Development Research, 84*(8), 1652-1663.

Waweru, H. K. (2024). Prevalence of *Plasmodium falciparum* antimalarial drugs resistance genetic markers in selected Lake Victoria Islands, Western Kenya. *JKUAT-COHES*.

Yahaya, F. N. (2022). Evaluation of the insecticide susceptibility status and molecular identities of Anopheles and Culex mosquitoes from selected areas within Ilorin metropolis. *Kwara State University (Nigeria)*.

Zhou S-F: Drugs behave as substrates, inhibitors and inducers of human cytochrome P450 3A4. Current drug metabolism 2008, 9(4):310-322.